

# Structure-Based Discovery of a Novel, Noncovalent Inhibitor of AmpC $\beta$ -Lactamase

Rachel A. Powers, Federica Morandi,  
and Brian K. Shoichet<sup>1</sup>

Department of Molecular Pharmacology  
and Biological Chemistry  
Northwestern University  
303 East Chicago Avenue  
Chicago, Illinois 60611

## Summary

$\beta$ -lactamases are the most widespread resistance mechanisms to  $\beta$ -lactam antibiotics, and there is a pressing need for novel, non- $\beta$ -lactam drugs. A database of over 200,000 compounds was docked to the active site of AmpC  $\beta$ -lactamase to identify potential inhibitors. Fifty-six compounds were tested, and three had  $K_i$  values of 650  $\mu$ M or better. The best of these, 3-[(4-chloroanilino)sulfonyl]thiophene-2-carboxylic acid, was a competitive noncovalent inhibitor ( $K_i = 26 \mu$ M), which also reversed resistance to  $\beta$ -lactams in bacteria expressing AmpC. The structure of AmpC in complex with this compound was determined by X-ray crystallography to 1.94 Å and reveals that the inhibitor interacts with key active-site residues in sites targeted in the docking calculation. Indeed, the experimentally determined conformation of the inhibitor closely resembles the prediction. The structure of the enzyme-inhibitor complex presents an opportunity to improve binding affinity in a novel series of inhibitors discovered by structure-based methods.

## Introduction

$\beta$ -lactams, such as penicillins and cephalosporins, are the most widely prescribed class of antibiotics (Figure 1A). In response to their extensive use and misuse, resistance to these drugs has become widespread. Their continued utility is threatened by the expression of  $\beta$ -lactamase enzymes, the most pervasive resistance mechanism to this class of antibiotics [1, 2]. These enzymes hydrolyze the lactam ring and render the antibiotic inactive against its original cellular targets, the cell wall transpeptidases.

In an effort to combat  $\beta$ -lactamase enzymes,  $\beta$ -lactamase inhibitors, such as clavulanic acid, and  $\beta$ -lactamase-resistant compounds, such as the third-generation cephalosporins, have been introduced (Figure 1B). Bacteria responded rapidly to these compounds because the compounds are themselves  $\beta$ -lactams. Existing resistance mechanisms, including  $\beta$ -lactamases, porin channel mutations, and sensor proteins, recognize and respond to the lactam ring functionality common to both substrates and inhibitors alike. These mechanisms are easily disseminated among bacteria, allowing resistance to these inhibitors to spread rapidly. Novel inhibi-

tors are required to avoid such preevolved resistance mechanisms. Inhibitors that do not chemically and structurally resemble  $\beta$ -lactams would not be hydrolyzed by  $\beta$ -lactamases and would not be recognized by sensor proteins that bind  $\beta$ -lactams and upregulate the expression of  $\beta$ -lactamases [3]. Additionally, a novel inhibitor may not be affected by porin channel mutants, which prevent  $\beta$ -lactams from accessing their cellular targets. An inhibitor that does not resemble a  $\beta$ -lactam minimizes the ability of bacteria to recruit existing resistance mechanisms, and novel mechanisms would need to be developed.

Several classes of non- $\beta$ -lactam inhibitors of  $\beta$ -lactamases have been identified. Transition-state analog inhibitors (Figure 1C), such as boronic acids and phosphonates, inhibit both class A and class C  $\beta$ -lactamases [4, 5]. Much effort has been devoted to improving the binding affinities of these molecules [3, 6–9]. One concern with both types of molecules is that they form covalent adducts with activated serine nucleophiles, potentially reducing their selectivity versus other serine active enzymes, such as serine proteases. A noncovalent inhibitor may be better suited as a candidate lead in drug development for this reason.

In an effort to identify a novel, noncovalent inhibitor of AmpC  $\beta$ -lactamase, we used a structure-based approach, beginning with a consensus map of “hot spots” on the enzyme. The consensus map was recently constructed from crystal structures of AmpC in complexes with 13 different ligands [10]. This map was used as a template in a molecular docking calculation to screen a database of over 200,000 small molecules for complementarity to the binding site. Based on the results of this screen, we ordered and tested 56 compounds for inhibition of AmpC; three of these had apparent  $K_i$  values of 650  $\mu$ M or better. The best of the three, 3-[(4-chloroanilino)sulfonyl]thiophene-2-carboxylic acid (compound 1; Figure 1D), was a competitive inhibitor of AmpC with a  $K_i$  value of 26  $\mu$ M (Table 1) and was able to reverse resistance in bacterial cell culture. The structure of AmpC in complex with compound 1 was determined to 1.94 Å resolution by X-ray crystallography and was found to closely resemble the docking prediction.

## Results

### Docking

The Northwestern University version [11, 12] of DOCK [13, 14] was used to screen the Available Chemicals Directory, a database of 229,810 commercially available small molecules, against the crystallographic structure of AmpC  $\beta$ -lactamase. The docking experiment incorporated information about hot spots identified on AmpC using a consensus overlay [10]. Two docking calculations, differing in the partial atomic charges assigned to several active site residues, were performed (see Ex-

**Key words:** antibiotic resistance; molecular docking; novel inhibitor discovery; structure-based drug design; X-ray structure

<sup>1</sup>Correspondence: b-shoichet@northwestern.edu

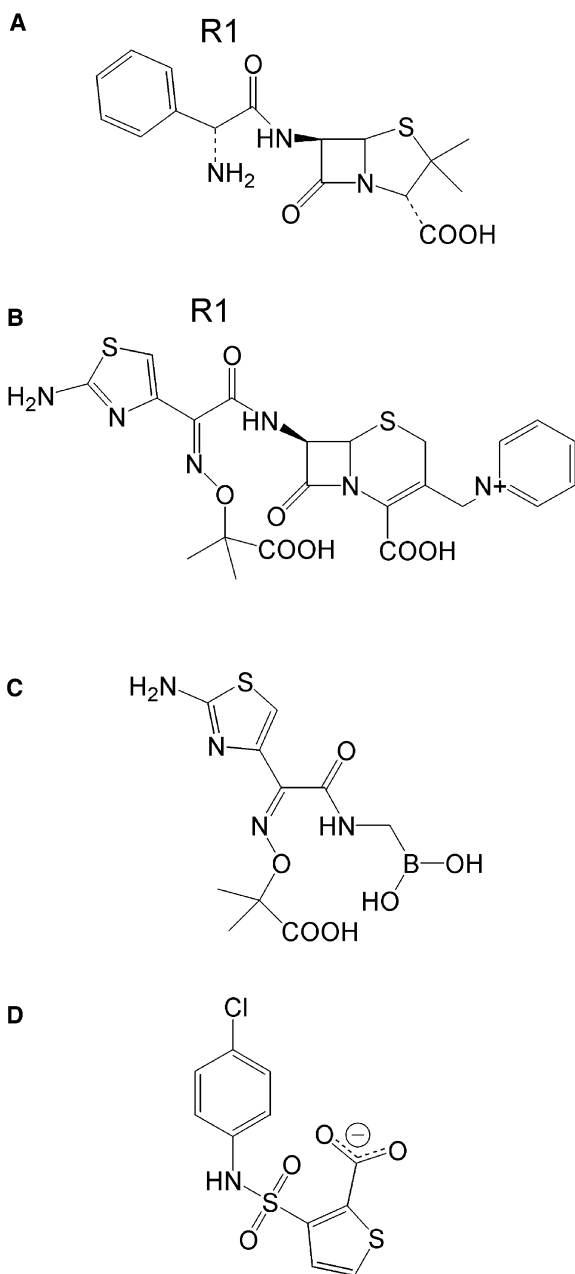


Figure 1. Comparison of the Chemical Structures of Several  $\beta$ -Lactamase Ligands

- (A) Ampicillin, a  $\beta$ -lactamase substrate.  
 (B) Ceftazidime, a  $\beta$ -lactamase-resistant molecule. The R1 side chain ubiquitous among  $\beta$ -lactams is labeled.  
 (C) A boronic acid transition-state analog inhibitor that contains the R1 side chain from ceftazidime [9].  
 (D) Compound 1, 3-[(4-chloroanilino) sulfonyl]thiophene-2-carboxylic acid, a novel, competitive inhibitor of  $\beta$ -lactamase.

perimental Procedures). The magnitudes of local partial atomic charges were increased, without changing the overall charges of the residues, in an effort to better capture the polarization thought to occur when ligands hydrogen bond to these residues. In our experience, DOCK and the Northwestern University version of this program used here underrepresent hydrogen bonding

and electrostatic contributions to binding. Increasing the partial atomic charges of receptor atoms in this way is an ad hoc solution to this problem and may not be generally useful. In this case, this solution did result in the emergence of putative ligands with improved polar complementarity to AmpC from the docking calculation.

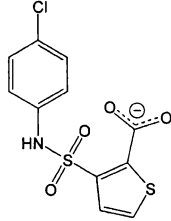
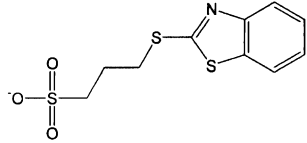
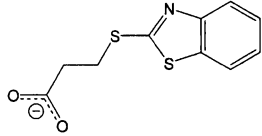
The 500 top-scoring molecules from each docking run were examined graphically for complementarity to the enzyme, for polar interactions with active site residues, and for agreement with binding sites identified in the consensus map. The lists were filtered for compounds that had been incorrectly represented in the database. From the two lists, we ordered and tested 56 compounds for inhibition of AmpC. Three molecules inhibited AmpC with  $K_i$  values of 650  $\mu$ M or better (compounds 1–3; Table 1). Compound 1 ranked 70th out of 229,810, compound 2 ranked 339th, and compound 3 ranked 370th in the hit list from the calculation using the larger dipoles; these compounds were not present in the other top 500 list. The DOCK-predicted conformations of these compounds and their interactions with AmpC are shown in Figure 2. Compound 1 is a competitive, reversible inhibitor with a  $K_i$  value of 26  $\mu$ M for AmpC, as determined by Lineweaver-Burk analysis (Figure 3). This compound was also tested for activity against the serine proteases  $\alpha$ -chymotrypsin,  $\beta$ -trypsin, and elastase (Table 1). Compound 1 showed no inhibition of trypsin and elastase at concentrations up to 4 mM and was approximately 50-fold more selective for AmpC over chymotrypsin.

Several intriguing interactions are observed between AmpC and compound 1 in the DOCK-predicted conformation (Figure 2A; Table 2). The carboxylate group is placed near the catalytic Ser64. One of the oxygens of the carboxylate interacts with  $O_\gamma$  of Ser64 and the main chain nitrogen of Ala318 and makes a close polar contact with the main chain oxygen of Ala318; the other oxygen interacts with the main chain nitrogen of Ala318 and Wat403, a conserved water molecule that was included in the docking experiment as part of the receptor. The thiophene ring of the inhibitor is placed in the hydrophobic binding site formed by Leu119 and Leu293. One of the sulfonamide oxygens interacts with  $O_\gamma$  of Ser64, and the other oxygen interacts with N $\delta$ 2 of Asn152. The nitrogen of the sulfonamide interacts with the main chain oxygen of Ala318. Finally, the chlorophenyl ring appears to stack with Tyr221. Several of these interactions agree with the consensus hot spot map; the Leu119/Leu293 hydrophobic patch is complemented with the thiophene ring, the amide recognition region defined by Asn152 and Ala318 hydrogen bonds to the sulfonamide, and one of the carboxylate oxygens is placed in the “oxyanion” [15] or “electrophilic” [3] hole, which can bind carbonyl and hydroxyl groups.

#### Crystallography

Subsequently, the structure of AmpC in complex with compound 1 was determined by X-ray crystallography to 1.94  $\text{\AA}$  resolution (Figure 4A; Table 3). The location of the inhibitor in each of the two active sites was unambiguously identified in the initial  $F_o - F_c$  difference maps when contoured at 3  $\sigma$ . In addition,  $F_o - F_c$  difference

Table 1. Kinetic Characterization of DOCK-Predicted Inhibitors of AmpC

Code	Structure	$K_i^a$ ( $\mu$ M) AmpC	$IC_{50}$ ( $\mu$ M) Chymotrypsin	$IC_{50}$ ( $\mu$ M) Trypsin	$IC_{50}$ ( $\mu$ M) Elastase
1		26	>1,200	>4,000	>4,000
2		318	ND <sup>b</sup>	ND	ND
3		646	ND	ND	ND

<sup>a</sup> Accurate to within 20%.

<sup>b</sup> Not determined.

electron density indicated the presence of a third inhibitor molecule located at the interface between the two molecules. Since this interface occurs only in AmpC crystals and not in solution, where AmpC is thought to be monomeric, we consider this site to be an artifact of crystallography. The electron density from a simulated-annealing omit map of the inhibitors in the refined model agreed well with the modeled conformation in each site (data not shown). The quality of the final model of the complex was analyzed with the program Procheck [16]; 92.5% of the nonproline, nonglycine residues are in the most-favored region of the Ramachandran plot (7.5% in the additionally allowed region). Comparison with the structure on which the docking calculation was performed showed that active site residues do not change much upon complex formation (rmsd for all atoms of Ser64, Lys67, Tyr150, Asn152, Tyr221, Lys315, and Ala318 was 0.22 Å for molecule 2 and 0.24 Å for molecule 1).

In the experimentally determined structure, compound 1 interacts with several active site residues (Figure 4B; Table 2). The carboxylate group is bound near Ser64, with one of its oxygens interacting with the main chain nitrogen and  $O_\gamma$  atoms of Ser64 and the main chain nitrogen of Ala318. The other oxygen of the carboxylate hydrogen bonds to Wat403 and, in molecule 2, to Wat481. The thiophene ring is within van der Waals distance to residues Leu119 and Leu293 (distances range from 4.2 to 4.6 Å), which form a hydrophobic patch on AmpC. One of the sulfonamide oxygen atoms hydrogen bonds to  $O_\gamma$  of Ser64 and  $N_\zeta$  of Lys67; the other interacts with  $N\delta_2$  of Asn152. The nitrogen atom of the sulfonamide group interacts with the main chain oxygen of Ala318. The chlorophenyl ring appears to be involved with quadrupole-quadrupole interactions with

Tyr221; the distance between the centroids of these two rings is between 5.5 and 5.8 Å, and the angle of interaction ranges from 91° to 94°.

The DOCK-predicted conformation of compound 1 closely resembles the experimentally determined structure (Figure 4C); the rmsd for all inhibitor atoms is 1.87 Å for molecule 2 and 1.75 Å for molecule 1 of the crystal structure. Much of the rms difference between the predicted and experimental structures arises from a rotation of the distal chlorophenyl ring about an internal bond and a rocking motion of the entire molecule about an axis defined by the hydrogen bonding groups that line the “bottom” side, i.e., the side facing the active site residues. Indeed, when only the inhibitor atoms that are involved in hydrogen bonds ( $N1$ ,  $O16$ ,  $O17$ ,  $O23$ , and  $O24$ ) are included in the analysis, the rmsd becomes 0.94 Å for molecule 2 and 0.95 Å for molecule 1.

In the crystal structure, the inhibitor is shifted and slightly rotated from the predicted conformation. Despite this shift, most of the interactions between AmpC and compound 1 in the predicted conformation are also observed in the experimental structure. Of the nine hydrogen bonding interactions observed in both monomers in the crystallographic complex, seven are also observed in the docked prediction (Table 2). Correspondingly, of the eight hydrogen bonding interactions predicted in the docked structure, only one is not observed crystallographically. For instance, the key interactions between the sulfonamide oxygen  $O17$  and Asn152 $N\delta_2$  and between the sulfonamide nitrogen  $N1$  and Ala318 $O$  are observed in both the experimental and predicted structures. On the other hand, interactions between the sulfonamide oxygen  $O16$  and Lys67 $N_\zeta$  and between the carboxylate oxygen and Ser64 $N$  are only observed in the crystal structure. The largest difference

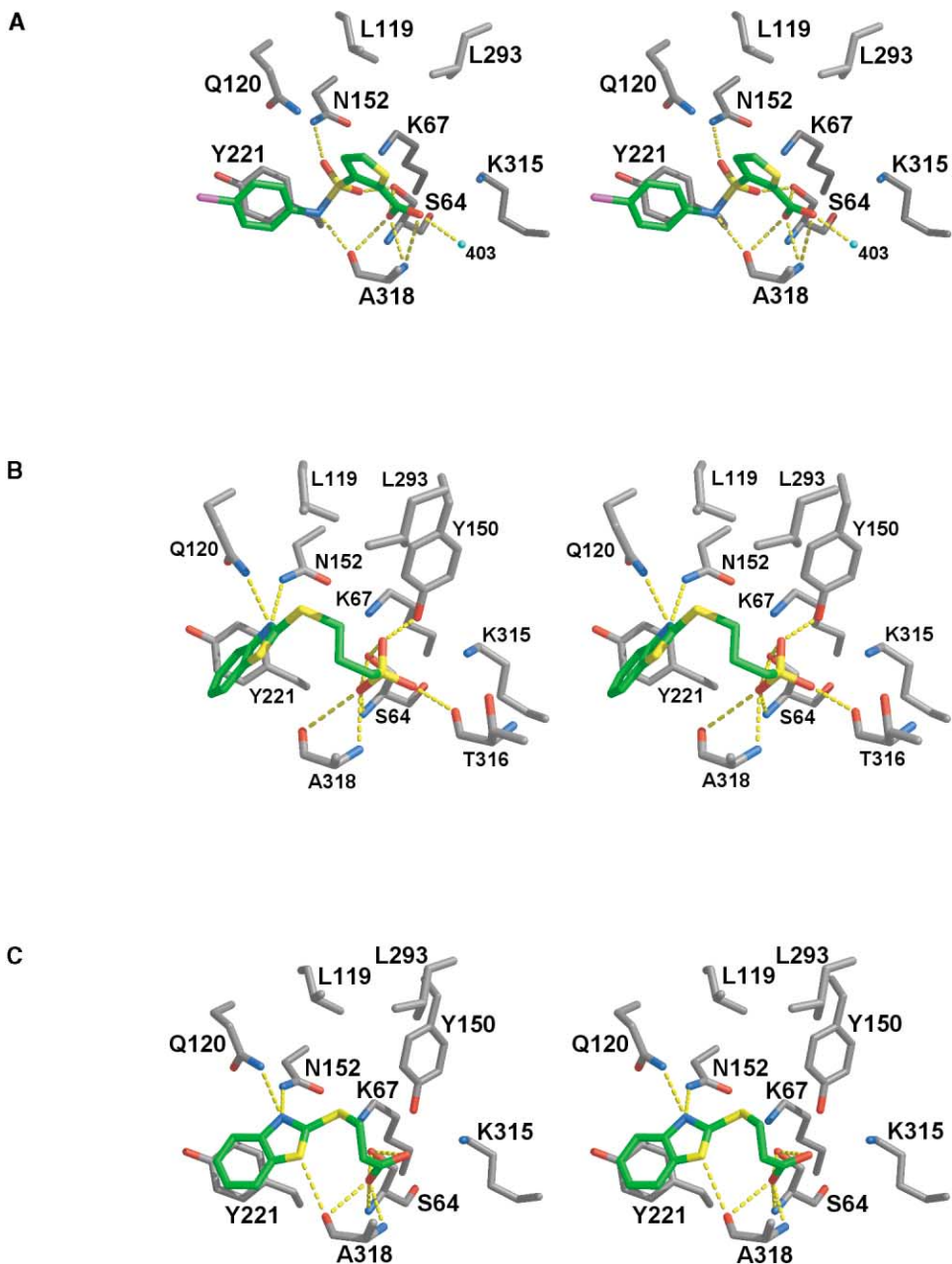


Figure 2. Stereo View of the Interactions Observed between AmpC and Compounds 1–3 in the DOCK-Predicted Orientations

(A) Compound 1.

(B) Compound 2.

(C) Compound 3.

Carbon atoms of the ligands, green; nitrogens, blue; oxygens, red; sulfurs, yellow; chlorines, magenta. Atomic interactions within hydrogen bonding distance are shown as dashed yellow lines. The cyan sphere labeled 403 in (A) represents Wat403; for clarity, Wat403 is not shown in (B) and (C). This figure and Figures 4B and 4C were generated with MidasPlus [31].

between the two structures is the orientation of the chlorophenyl ring; in the crystal structure, this ring has rotated approximately  $60^\circ$ , as measured by the dihedral angle around S13, N1, C2, and C3. This ring now interacts in a more edge to face manner with Tyr221, presumably making quadrupole-quadrupole interactions with Tyr221, instead of the parallel face to face interaction predicted by docking.

### Microbiology

We investigated the ability of compound 1 to potentiate the activity of a  $\beta$ -lactam against a strain of resistant bacteria that overexpresses AmpC. In bacterial cell culture, the potency of ampicillin when given in combination with compound 1 is increased 4-fold, reducing its minimum inhibitory concentration (MIC) to  $128 \mu\text{g/ml}$  (Table 4). The MIC of ampicillin in the absence of com-

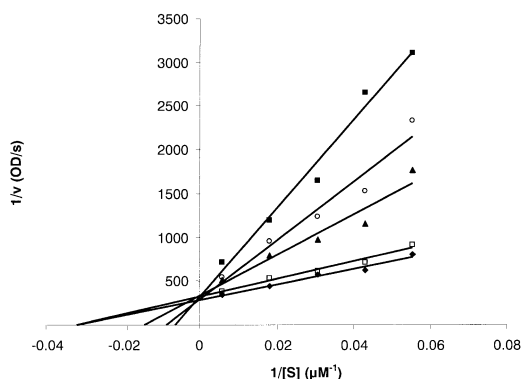


Figure 3. Lineweaver-Burk Plot of the Inhibition of AmpC by Compound 1

Inhibitor concentrations were 0  $\mu\text{M}$  ( $\blacklozenge$ ), 15  $\mu\text{M}$  ( $\square$ ), 60  $\mu\text{M}$  ( $\blacktriangle$ ), 105  $\mu\text{M}$  ( $\circ$ ), and 150  $\mu\text{M}$  ( $\blacksquare$ ). Each data point is the average of three experimental observations. The  $K_i$  value is 26  $\mu\text{M}$ .

Compound 1 was 512  $\mu\text{g/ml}$ . At this concentration compound 1 alone had no measurable antibiotic activity.

#### Structure-Activity Relationship of Compound 1

Several inhibitor moieties appeared to be key to enzyme recognition based on the docking score and the crystal structure. To investigate the energetic importance of the predicted and observed interactions, six analogs of compound 1 were tested for inhibition (compounds 4–9; Table 5). The carboxylate group of compound 1, which hydrogen bonds with residues in the oxyanion or electrophilic hole of AmpC, appears to be essential; binding

was abolished when this group was replaced with a methyl ester (compound 5) or a nitro group (compound 9). Switching the atom order of the sulfonamide group (compound 4), which hydrogen-bonds with Asn152 and Ala318, reduced affinity 3-fold. Disruption of the proton-donating ability of the sulfonamide nitrogen (compound 6) abolished binding. The addition of a piperidine ring to the distal aryl ring (compound 7) increased affinity, but only 2-fold, consistent with this substitution occurring in a solvent-exposed region of the binding site.

#### Discussion

The most compelling result to emerge from this study is the identification of a novel, competitive, noncovalent inhibitor of AmpC  $\beta$ -lactamase. All previously known inhibitors form covalent adducts with the catalytic Ser64; with few exceptions [3, 17], all are either  $\beta$ -lactams [18–21] or molecules that mimic  $\beta$ -lactams [9, 22]. Conversely, compounds 1–3 form noncovalent complexes using chemistry dissimilar to that found in classical inhibitors to bind to key substrate-recognition residues in the AmpC active site.

Although compound 1 does not resemble a  $\beta$ -lactam by any standard classification scheme, it recapitulates some familiar themes of  $\beta$ -lactam recognition by  $\beta$ -lactamases when viewed in the context of its complex with AmpC. The sulfonamide group of compound 1 binds in the site that recognizes the ubiquitous C6(7)-amide found in the R1 side chains of  $\beta$ -lactams, where it hydrogen bonds to two of the amide-recognizing residues, Asn152 and Ala318 (Figure 4B). Although these

Table 2. Interactions in the Crystallographic and DOCK-Predicted Complexes of AmpC with 1

Interaction	Distance (Å)		
	AmpC/1		DOCK Prediction
	Molecule 1	Molecule 2	
S64N-O23	3.0	2.9	3.6
S64O $\gamma$ -O23	2.9	2.8	3.0
A318O-O23	2.9	3.0	2.7
A318N-O23	2.8	2.9	2.6
A318N-O24	3.4	3.4	3.1
Wat403 <sup>a</sup> -O24	2.9	2.7	2.5
Wat481-O24	—	2.7	—
S64O $\gamma$ -O16	2.7	2.7	2.4
K67N $\zeta$ -O16	3.1	3.1	4.3
N152N $\delta$ 2-O17	2.7	2.7	2.6
A318O-N1	2.7	2.7	2.6
Centroid of Tyr221-centroid of phenyl ring of 1	5.5	5.8	4.6

<sup>a</sup> Wat403 is called Wat401 in molecule 1 of the asymmetric unit.

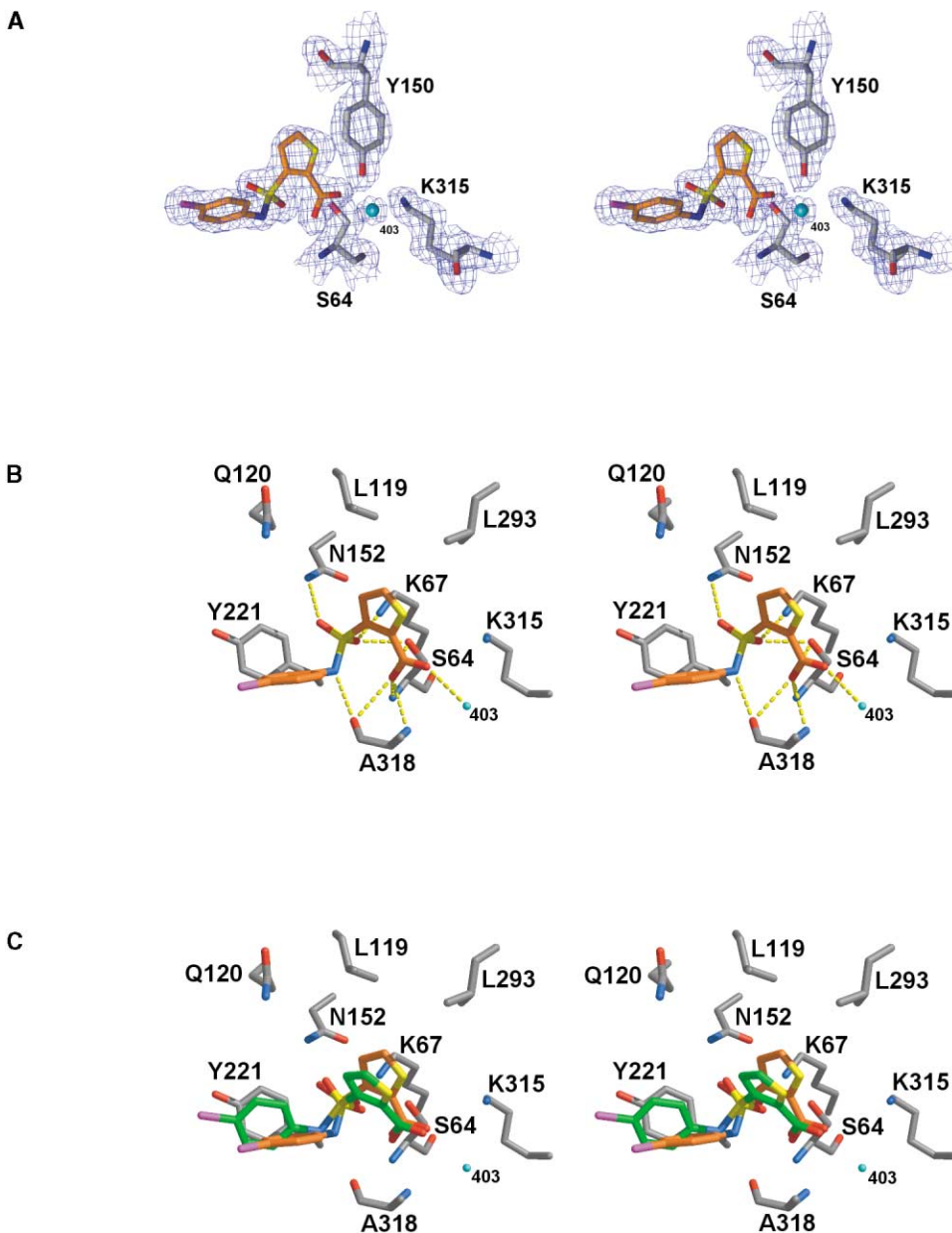


Figure 4. Stereo View of the Active Site Region of the AmpC/1 Complex Determined to 1.94 Å Resolution

(A) The 2F<sub>o</sub> - F<sub>c</sub> electron density map is shown in blue, contoured at 1.0 σ. This figure was made with SETOR [41].

(B) Interactions observed between AmpC and compound 1 in the crystallographic complex. Cyan spheres represent water molecules. Dashed yellow lines indicate hydrogen bonds. Atoms are colored as in Figure 2, except that the carbon atoms of compound 1 are colored orange.

(C) Overlay of the docked and crystallographic conformations of compound 1 in the AmpC site. Carbon atoms of compound 1 in the docked conformation, green; carbon atoms of compound 1 in the crystal structure, orange.

hydrogen bonds resemble those made by the amide functionality of β-lactams, the atom order of the sulfonamide group in compound 1 is the reverse of the amide found in the R1 side chains of β-lactams (Figures 1A and 1B). Additionally, one of the oxygen atoms of the carboxylate group of compound 1 binds in the oxanion [15] or electrophilic [3] hole of the β-lactamase, hydrogen bonding to the main chain nitrogens of Ser64 and Ala318 (Figure 4B). This interaction resembles those made by the carbonyl oxygen atom of β-lactams with these residues in several acyl-enzyme complexes of

β-lactamases with β-lactams [18, 20, 21, 23–25]. Finally, the terminal chlorophenyl ring of compound 1 stacks with the conserved residue Tyr221. This interaction is similar to those made by the aryl rings found in β-lactams such as cephalothin [26], loracarbef [20], and ceftazidime [25].

It is interesting to consider how many of these interactions were captured in the docking prediction that led to the discovery of this inhibitor. The rmsd between the docked and experimental structures varied from 1.7–1.9 Å, depending on which molecule in the asymmetric

Table 3. Crystallographic Summary for the Complex of AmpC/1

	AmpC/1
Cell constants ( $\text{\AA}$ ; $^\circ$ )	a = 118.67 b = 76.42 c = 97.90; $\beta$ = 116.63
Resolution ( $\text{\AA}$ )	1.94 (1.99–1.94) <sup>a</sup>
Unique reflections	56,580
Total observations	208,148
R <sub>merge</sub> (%)	5.5 (31.5)
Completeness (%) <sup>b</sup>	97.8 (95.1)
$\langle I \rangle / \langle \sigma_I \rangle$	14.5 (4.2)
Resolution range for refinement ( $\text{\AA}$ )	20–1.94
Number of protein residues	713
Number of water molecules	352
Rmsd bond lengths ( $\text{\AA}$ )	0.009
Rmsd bond angles ( $^\circ$ )	1.5
R factor (%)	17.3
R <sub>free</sub> (%) <sup>c</sup>	20.7
Average B factor, protein atoms ( $\text{\AA}^2$ ; molecule 1)	23.8
Average B factor, protein atoms ( $\text{\AA}^2$ ; molecule 2)	23.6
Average B factor, inhibitor atoms ( $\text{\AA}^2$ ; molecule 1)	29.8
Average B factor, inhibitor atoms ( $\text{\AA}^2$ ; molecule 2)	37.1
Average B factor, water molecules ( $\text{\AA}^2$ )	31.1

<sup>a</sup> Highest resolution shell boundaries in parentheses. Subsequent values in parentheses are for that shell.

<sup>b</sup> Fraction of theoretically possible reflections observed.

<sup>c</sup> R<sub>free</sub> was calculated with 5% of reflections set aside randomly.

unit was used in the comparison. Notwithstanding this quantitative difference, the two structures qualitatively and visually resemble each other closely. Of the nine hydrogen bonds observed in the crystal structure, seven were predicted in the docked complex, and both of the two major nonpolar interactions were predicted. The major difference between the docked and experimental configurations is the rotation of the chlorophenyl ring by 60° that results in a herringbone, or edge to face, stacking interaction between this ring and Tyr221, rather than a face to face stacking interaction.

The solvation-corrected docking energy score may be apportioned among the atoms of the ligand using the atom by atom partitioning of the AMSOL solvation and the docking energy calculations. These scores suggest that the carboxylate and sulfonamide functionalities of compound 1 are key binding determinants. Whereas these atomic energies are not quantitative, they can be useful as qualitative guides to subsequent experiments. Several analogs were tested to explore the importance of these groups to binding affinity (Table 5). Substitution of the carboxylate with a neutral isostere abolished inhibition. Switching the order of the sulfonamide diminished inhibition 3-fold, suggesting that this unusual amide arrangement is nevertheless preferred in this noncovalent inhibitor. These effects seem sensible,

Table 4. Synergy of Compound 1 with the  $\beta$ -Lactam Ampicillin Against AmpC Producing *E. coli*

	Resistant Cells MIC <sup>a</sup> ( $\mu\text{g/ml}$ )	Sensitive Cells MIC ( $\mu\text{g/ml}$ )
Ampicillin	512	4
Ampicillin/1 <sup>b</sup>	128	ND <sup>c</sup>
Compound 1	>512	ND

<sup>a</sup> Minimum inhibitory concentration.

<sup>b</sup> The ratio of ampicillin to inhibitor was 1:2.

<sup>c</sup> Not determined.

since, in the crystal structure, these groups hydrogen bond extensively with the enzyme; any disruption of these interactions would be expected to adversely affect affinity.

In our docking experiment, 13 previously determined structures of AmpC/ligand complexes were used to flag hot spots for binding and to identify tightly bound water molecules [10]. Consensus binding sites were identified for an amide/aryl site, a carbonyl/hydroxyl site, a hydroxyl site, a carboxylate site, and a hydrophobic site. In their docked complexes, the three new inhibitors exploited these hot spots (Figure 2); for example, an oxygen atom from the carboxylate group of compounds 1 and 3 and the sulfate group of compound 2 was predicted to bind in the carbonyl/hydroxyl site, and the hydrophobic site was complemented with hydrophobic portions of each of these compounds. Intriguingly, the new inhibitors took advantage of the consensus hot spots using functionality not found in the 13 ligands used to identify the hot spots in the first place. For instance, compound 1 placed a sulfonamide in the amide recognition site of AmpC, whereas none of the 13 placed a sulfonamide there. Compound 1 used a carboxylate group to bind in the oxyanion or electrophilic hole of the  $\beta$ -lactamase, which had originally been defined as recognizing only carbonyl or hydroxyl groups. Compounds 2 and 3 placed a benzoaminothiazole ring in the amide/aryl recognition site, but this functionality was not represented by any of the 13 ligands.

The inclusion of bound water molecules in our docking experiment also came out of analysis of the 13 previous complexes used to identify the consensus hot spots. Water molecules included as part of the receptor influence what ligands are identified in a docking calculation, both by acting as a point of interaction for the docked molecules and by excluding them from occupying the volume that the water itself occupies. Consequently, there is much interest in how water influences the results of docking and structure-based design calculations [27–

Table 5. Kinetic Characterization of Analogs of 1

Code	Structure	$K_i$ ( $\mu\text{M}$ ) AmpC
1		26
4		60
5		>>100 <sup>a</sup>
6		>>100 <sup>a</sup>
7		14
8		64
9		>>100 <sup>a</sup>

<sup>a</sup>No detectable inhibition at 100  $\mu\text{M}$  concentration of compound.

29]. Based on the analysis of waters conserved in AmpC structures, we treated three waters as nondisplaceable parts of the receptor: Wat403, Wat404, and Wat405. Wat404 and Wat405 are relatively distant from the site of docking and will not be considered further. Wat403 is at the center of the active site (Figure 2A). We used this water in the docking calculation because it is highly conserved in all AmpC structures (present in 29 of 30 molecules that we previously examined [10]) and because it is well coordinated by the enzyme. The inclusion of this water appears to have influenced that calculation beneficially, as it hydrogen bonds with the inhibitor in both the docked and the crystallographic structures of compound 1 bound to AmpC.

Compound 1 inhibits AmpC with a  $K_i$  value of 26  $\mu\text{M}$ . Compared to more-traditional covalent inhibitors of AmpC, this is a modest level of inhibition. Nevertheless, the compound holds promise as a lead for drug discovery; it explores novel chemical functionality, which it uses to complement key recognition residues of the  $\beta$ -lactamase. The recognition “code” of the AmpC structure appears to be plastic [3]; not only are  $\beta$ -lactams recognized by highly conserved active site residues, but compounds bearing very different functionality can also bind. Notwithstanding its modest level of inhibition, compound 1 reversed antibiotic resistance in bacterial cell culture. The compound was selective for AmpC; it did not significantly inhibit related serine proteases in counterscreens. Finally, it is relatively “drug-like,” passing four of four Lipinski rules [30], and has several sites for synthetic elaboration. The ability to discover such inhibitors through structure-based techniques and the correspondence between the docking prediction and the experimental result hold promise for the development of this and other families of novel inhibitors of serine  $\beta$ -lactamases. Such novel inhibitors are much needed as  $\beta$ -lactamase-mediated antibiotic resistance continues to spread among bacterial pathogens.

### Biological Implications

$\beta$ -lactamase enzymes are the most widespread resistance mechanisms to  $\beta$ -lactam antibiotics. Clinically used inhibitors for these enzymes resemble substrates; both contain a  $\beta$ -lactam ring. For this reason, resistance develops rapidly because mechanisms that depend on recognition of the lactam ring already exist. A novel inhibitor may evade such mechanisms, and, most importantly, it would not be hydrolyzed by  $\beta$ -lactamases. In an effort to discover novel inhibitors, we screened a database of small molecules for complementarity to the enzyme active site. Three novel inhibitors were identified; the best was a reversible, competitive inhibitor, with a  $K_i$  of 26  $\mu\text{M}$ . The structure of the complex between AmpC and this inhibitor was determined by X-ray crystallography and revealed that the inhibitor complements the active site well through interactions with several key active-site residues. These interactions resemble those observed between the enzyme and  $\beta$ -lactams and yet, at the same time, are fundamentally different. It is only in the context of the complex with the enzyme that any similarity can be discerned between compound 1 and

a  $\beta$ -lactam. This suggests that the “code” for recognition by AmpC is plastic, and this plasticity can be used for inhibitor discovery. The identification of a novel, noncovalent inhibitor along with the structure of its complex with AmpC provides an opportunity for structure-based design efforts to improve binding affinity.

## Experimental Procedures

### Docking

The Available Chemicals Directory was screened against molecule 2 of native AmpC (Protein Data Bank entry 1KE4) using the Northwestern University version [11, 12] of DOCK [13, 14]. To prepare the site for docking, we removed all water and ion molecules, except for Wat403, Wat404, and Wat405. These specific water molecules were included as part of the receptor because they are observed in nearly all AmpC structures and are expected to be tightly bound. Protonation of receptor residues and water molecules was done with Sybyl (Tripos, St. Louis). Positions of some protons were then rotated manually to more appropriate orientations using MidasPlus [31]. The sphere set used was based on ligand atom positions from an ensemble of structures of nine boronic acid inhibitors and four  $\beta$ -lactam molecules determined in complex with AmpC  $\beta$ -lactamase by X-ray crystallography [10]. This resulted in the cluster of 73 spheres, each of which represented a ligand atom position observed in the X-ray structures used in the docking calculation. The spheres were labeled based on the chemical functionality of the ligand atoms they represented [32]. Force field and electrostatic grids were calculated with CHEMGRID [33] and DelPhi [34], respectively. DISTMAP was used to calculate the excluded volume grid [33].

Calculated interaction energies in the docking calculation were corrected for ligand desolvation [12] (Wei and B.K.S., unpublished data) using AMSOL [35], which was also used to calculate ligand partial atomic charges. Each orientation of the docked ligands was refined with 100 iterations of rigid-body minimization [14]. The distance tolerance parameter for calculating orientations was set to 1.2 Å. The ligand and receptor bin sizes were each 0.2 Å, and ligand and receptor overlap were also each 0.2 Å. Chemical matching was used to specify how ligand atoms were to be matched to the spheres [32]. To improve hydrogen bonding opportunities between active site residues and the ligands, the absolute magnitude of the partial atomic charges of the following active site residues were increased by 0.4 units and, in a second docking calculation, by 0.8 units: Ser64O $\gamma$  and HO $\gamma$ ; Gln120O $\epsilon$ 1, HNe1, and HNe2; Tyr150OH and HOH; Asn152O $\delta$ 1, HN $\delta$ 1, and HN $\delta$ 2; Tyr221OH and HOH; Asn289O $\delta$ 1, HN $\delta$ 1, and HN $\delta$ 2; Thr316O $\gamma$ 1 and HO $\gamma$ ; Ala318O and HN; Asn343O $\delta$ 1, HN $\delta$ 1, and HN $\delta$ 2; Asn346O $\delta$ 1, HN $\delta$ 1, and HN $\delta$ 2. For the asparagine and glutamine residues, the charge increase was split among the protons on the amide groups. The 500 top-scoring molecules from each docking run were displayed with MidasPlus [31]. From these two lists, we ordered and tested 56 compounds for their ability to inhibit AmpC.

### Enzymology

AmpC from *Escherichia coli* was expressed and purified to homogeneity as described [3]. Compound 1, 3-[[4-(4-chloroanilino)sulfonyl]thiophene-2-carboxylic acid, compound 4, 2-methyl-4-[[4-(4-methylphenyl)sulfonyl]amino]thiophene-3-carboxylic acid, compound 5, methyl 3-[[4-(4-chloroanilino)sulfonyl]thiophene-2-carboxylate, compound 6, 3-[[4-(3-chloro-5-(trifluoromethyl)pyridin-2-yl)piperazino]sulfonyl]thiophene-2-carboxylate, compound 7, 3-[[2-(piperidinoanilino)sulfonyl]thiophene-2-carboxylic acid, and compound 8, 2,5-dimethyl-4-(2-thienylaminosulfonyl)furan-3-carboxylic acid, were obtained from Maybridge Chemical (Cornwall, UK). Compound 2, 3-(2-benzothiazolythio)-1-propanesulfonic acid, and compound 9, N-(4-methoxyphenyl)-2-nitro-benzenesulfonamide, were obtained from Aldrich Chemical (Milwaukee, WI). Compound 3, 3-(2-benzothiazolythio)propionic acid, was obtained from TCI America (Portland, OR). All were used without further purification. Kinetic measurements with AmpC were performed in 50 mM Tris buffer (pH 7.0) using nitrocefin as a substrate. The  $K_m$  of nitrocefin for AmpC in this buffer was determined to be 127  $\mu$ M. Reactions were initiated by

the addition of 0.875 nM enzyme and monitored in methacrylate cuvettes. No incubation effect was detected for any compound.  $IC_{50}$  values were determined at 200  $\mu$ M substrate concentration.  $K_i$  values for the compounds were obtained by comparison of progress curves in the presence and absence of inhibitor [36]. Sufficient inhibitor was used to give at least 50% inhibition. For compound 1, a  $K_i$  of 26  $\mu$ M, consistent with the value of 23  $\mu$ M determined by progress curve analysis, was determined by Lineweaver-Burk analysis of multiple substrate and inhibitor concentrations (Figure 3); a  $K_i$  value of 28  $\mu$ M was determined from nonlinear fitting of the same data (data not shown). We note that all compounds discussed here were well behaved kinetically and do not fall into the category of aggregation-based promiscuous inhibitors that we have recently described [37].

The selectivity of compound 1 for AmpC was determined by measuring its activity against  $\alpha$ -chymotrypsin (bovine pancreatic),  $\beta$ -trypsin (bovine pancreatic), and elastase (porcine pancreatic), all from Sigma (St. Louis). The substrates for  $\alpha$ -chymotrypsin (succinyl-alanyl-alanyl-pro-phe-p-nitroanilide) and  $\beta$ -trypsin (N-benzoyl-L-arginine ethyl ester, BAEE) were also purchased from Sigma. The elastase substrate (elastase substrate 1, MeOSuc-Ala-Ala-Pro-Val-p-nitroanilide) was purchased from Calbiochem (San Diego, CA). Substrates were diluted from 10 mM stock solutions in dimethylsulfoxide (DMSO), and all reactions were performed in 50 mM Tris buffer (pH 7.0) 25°C. For  $\alpha$ -chymotrypsin, 200  $\mu$ M substrate was used; the reactions were initiated by the addition of 10  $\mu$ l of a 0.1 mg/ml enzyme stock solution and monitored at 410 nm. For  $\beta$ -trypsin, 200  $\mu$ M BAEE was used; the reactions were initiated by the addition of 5  $\mu$ l of a 0.2 mg/ml enzyme stock solution and monitored at 260 nm. For elastase, 640  $\mu$ M substrate was used; the reactions were initiated by the addition of 30  $\mu$ l of a 0.2 mg/ml enzyme stock solution and monitored at 385 nm. Initial rate fits to the absorbance data for the first 150 s of each reaction were used to determine reaction velocities.

### Crystal Growth and Structure Determination

Cocrystals of AmpC/1 were grown by vapor diffusion in hanging drops equilibrated over 1.7 M potassium phosphate buffer (pH 8.7) using microseeding techniques. The initial concentration of protein in the drop was 95  $\mu$ M, and the concentration of the inhibitor was 1.2 mM. The inhibitor was added to the crystallization drop in a 4% DMSO, 1.7 M potassium phosphate buffer (pH 8.7) solution. Crystals appeared within 3–5 days after equilibration at 23°C.

Data were measured from a single crystal on the DND-CAT beamline (5IDB) of the Advanced Photon Source at Argonne National Lab at 100 K using a Mar CCD detector. Prior to data collection, the cocrystal of AmpC/1 was immersed in a cryoprotectant solution of 20% sucrose, 1.2 mM compound 1, and 1.7 M potassium phosphate (pH 8.7) for about 20 s and then flash cooled in liquid nitrogen.

Reflections were indexed, integrated, and scaled using the HKL package [38] (Table 3). The space group was C2, with two AmpC molecules in the asymmetric unit. The structure of the complex was determined using a native apo AmpC structure (Protein Data Bank entry 1KE4) [10], with water molecules and ions removed, as the initial phasing model. The structure was refined using the maximum-likelihood target in CNS and included simulated-annealing, positional, and individual temperature factor refinement with a bulk solvent correction [39].  $\sigma_A$ -weighted electron density maps were calculated with CNS and used in steps of manual rebuilding with the program O [40]. The inhibitor was built into the initial observed difference density in each active site of the asymmetric unit, and the structure of the complex was further refined using CNS (Table 3). In the final model, molecule 1 contained 355 residues, molecule 2 contained 358 residues, and there are 352 water molecules. Electron density for a third inhibitor molecule was observed between the two AmpC molecules, and the inhibitor was modeled into this electron density as well.

### Microbiology Experiments

To test the inhibitory activity of compound 1, the compound was dissolved in DMSO at a concentration of 50 mM and dilutions were performed using Luria Broth growth medium. An adequate final concentration at which to determine the MIC was obtained where the concentration of DMSO was maintained below 5%. The MIC of

the  $\beta$ -lactam ampicillin, in the presence and absence of compound 1, was determined against JM109 *E. coli* expressing AmpC.

#### Acknowledgments

This work was supported by GM59953 and GM63815 from the National Institutes of Health (to B.K.S.) and by a predoctoral fellowship from the American Chemical Society Division of Medicinal Chemistry and Bristol-Myers Squibb (to R.A.P.). We thank G. Minasov and X. Wang for collecting the crystallographic data reported here. We thank B. Beadle, P. Focia, J. Irwin, and S. McGovern for reading this manuscript. The DuPont-Northwestern-Dow Collaborative Access Team at the APS is supported by E.I. DuPont de Nemours and Company, the Dow Chemical Company, the National Science Foundation, and the state of Illinois.

Received: March 12, 2002

Revised: June 11, 2002

Accepted: June 13, 2002

#### References

1. Neu, H.C. (1992). The crisis in antibiotic resistance. *Science* 257, 1064–1073.
2. Davies, J. (1994). Inactivation of antibiotics and the dissemination of resistance genes. *Science* 264, 375–382.
3. Powers, R.A., Blazquez, J., Weston, G.S., Morosini, M.I., Baquero, F., and Shoichet, B.K. (1999). The complexed structure and antimicrobial activity of a non- $\beta$ -lactam inhibitor of AmpC beta-lactamase. *Protein Sci.* 8, 2330–2337.
4. Rahil, J., and Pratt, R.F. (1991). Phosphonate monoester inhibitors of class A beta-lactamases. *Biochem. J.* 275, 793–795.
5. Beesley, T., Gascoyne, N., Knott-Hunziker, V., Petursson, S., Waley, S.G., Jaurin, B., and Grundstrom, T. (1983). The inhibition of class C beta-lactamases by boronic acids. *Biochem. J.* 209, 229–233.
6. Rahil, J., and Pratt, R.F. (1993). Structure-activity relationships in the inhibition of serine beta-lactamases by phosphonic acid derivatives. *Biochem. J.* 296, 389–393.
7. Strynadka, N.C., Martin, R., Jensen, S.E., Gold, M., and Jones, J.B. (1996). Structure-based design of a potent transition state analogue for TEM-1 beta-lactamase. *Nat. Struct. Biol.* 3, 688–695.
8. Ness, S., Martin, R., Kindler, A.M., Paetzel, M., Gold, M., Jensen, S.E., Jones, J.B., and Strynadka, N.C. (2000). Structure-based design guides the improved efficacy of deacylation transition state analogue inhibitors of TEM-1 beta-lactamase. *Biochemistry* 39, 5312–5321.
9. Caselli, E., Powers, R.A., Blaszczak, L.C., Wu, C.Y., Prati, F., and Shoichet, B.K. (2001). Energetic, structural, and antimicrobial analyses of beta-lactam side chain recognition by beta-lactamases. *Chem. Biol.* 8, 17–31.
10. Powers, R.A., and Shoichet, B.K. (2002). Structure-based approach for binding site identification on AmpC beta-lactamase. *J. Med. Chem.*, in press.
11. Lorber, D.M., and Shoichet, B.K. (1998). Flexible ligand docking using conformational ensembles. *Protein Sci.* 7, 938–950.
12. Shoichet, B.K., Leach, A.R., and Kuntz, I.D. (1999). Ligand solvation in molecular docking. *Proteins* 34, 4–16.
13. Kuntz, I.D., Blaney, J.M., Oatley, S.J., Langridge, R., and Ferrin, T.E. (1982). A geometric approach to macromolecule-ligand interactions. *J. Mol. Biol.* 161, 269–288.
14. Meng, E.C., Gschwend, D.A., Blaney, J.M., and Kuntz, I.D. (1993). Orientational sampling and rigid-body minimization in molecular docking. *Proteins* 17, 266–278.
15. Murphy, B.P., and Pratt, R.F. (1988). Evidence for an oxyanion hole in serine beta-lactamases and DD-peptidases. *Biochem. J.* 256, 669–672.
16. Laskowski, R.A., MacArthur, M.W., Moss, D.S., and Thornton, J.M. (1993). PROCHECK: a program to check the stereochemical quality of protein structures. *J. Appl. Crystallogr.* 26, 283–291.
17. Tondi, D., Powers, R.A., Caselli, E., Negri, M.C., Blazquez, J., Costi, M.P., and Shoichet, B.K. (2001). Structure-based design and in-parallel synthesis of inhibitors of AmpC beta-lactamase. *Chem. Biol.* 8, 593–611.
18. Oefner, C., D'Arcy, A., Daly, J.J., Gubernator, K., Charnas, R.L., Heinze, I., Hubschwerlen, C., and Winkler, F.K. (1990). Refined crystal structure of beta-lactamase from *Citrobacter freundii* indicates a mechanism for beta-lactam hydrolysis. *Nature* 343, 284–288.
19. Maveyraud, L., Mourey, L., Kotra, L.P., Pedelacq, J.D., Guillet, V., Mobashery, S., and Samama, J.P. (1998). Structural basis for clinical longevity of carbapenem antibiotics in the face of challenge by the common class A beta-lactamases from the antibiotic-resistant bacteria. *J. Am. Chem. Soc.* 120, 9748–9752.
20. Patera, A., Blaszczak, L.C., and Shoichet, B.K. (2000). Crystal structures of substrate and inhibitor complexes with AmpC beta-lactamase: possible implications for substrate-assisted catalysis. *J. Am. Chem. Soc.* 122, 10504–10512.
21. Fozze, E., Vanhove, M., Dive, G., Sauvage, E., Frere, J.M., and Charlier, P. (2002). Crystal structures of the *Bacillus licheniformis* BS3 class A beta-lactamase and of the acyl-enzyme adduct formed with cefoxitin. *Biochemistry* 41, 1877–1885.
22. Lobkovsky, E., Billings, E.M., Moews, P.C., Rahil, J., Pratt, R.F., and Knox, J.R. (1994). Crystallographic structure of a phosphonate derivative of the *Enterobacter cloacae* P99 cephalosporinase: mechanistic interpretation of a beta-lactamase transition-state analog. *Biochemistry* 33, 6762–6772.
23. Chen, C.C., and Herzberg, O. (1992). Inhibition of beta-lactamase by clavulanate. Trapped intermediates in cryocrystallographic studies. *J. Mol. Biol.* 224, 1103–1113.
24. Strynadka, N.C., Adachi, H., Jensen, S.E., Johns, K., Sielecki, A., Betzel, C., Sutoh, K., and James, M.N. (1992). Molecular structure of the acyl-enzyme intermediate in beta-lactam hydrolysis at 1.7 Å resolution. *Nature* 359, 700–705.
25. Powers, R.A., Caselli, E., Focia, P.J., Prati, F., and Shoichet, B.K. (2001). Structures of ceftazidime and its transition-state analogue in complex with AmpC beta-lactamase: implications for resistance mutations and inhibitor design. *Biochemistry* 40, 9207–9214.
26. Beadle, B.M., Trehan, I., Focia, P.J., and Shoichet, B.K. (2002). Structural milestones in the reaction pathway of an amide hydrolase: substrate, acyl, and product complexes of cephalothin with AmpC beta-lactamase. *Structure* 10, 413–442.
27. Minke, W.E., Diller, D.J., Hol, W.G., and Verlinde, C.L. (1999). The role of waters in docking strategies with incremental flexibility for carbohydrate derivatives: heat-labile enterotoxin, a multivalent test case. *J. Med. Chem.* 42, 1778–1788.
28. Rarey, M., Kramer, B., and Lengauer, T. (1999). The particle concept: placing discrete water molecules during protein-ligand docking predictions. *Proteins* 34, 17–28.
29. Lengauer, T., and Zimmer, R. (2000). Protein structure prediction methods for drug design. *Brief. Bioinform.* 1, 275–288.
30. Lipinski, C.A., Lombardo, F., Dominy, B.W., and Feeney, P.J. (1997). Experimental and computational approaches to estimate solubility and permeability in drug discovery and development settings. *Adv. Drug Deliv. Rev.* 23, 3–25.
31. Ferrin, T.E., Huang, C.C., Jarvis, L.E., and Langridge, R. (1988). The MIDAS display system. *J. Mol. Graph.* 6, 13–27.
32. Shoichet, B.K., and Kuntz, I.D. (1993). Matching chemistry and shape in molecular docking. *Protein Eng.* 6, 723–732.
33. Meng, E.C., Shoichet, B.K., and Kuntz, I.D. (1992). Automated docking with grid-based energy evaluation. *J. Comput. Chem.* 13, 505–524.
34. Gilson, M.K., and Honig, B.H. (1987). Calculation of electrostatic potentials in an enzyme active site. *Nature* 330, 84–86.
35. Li, J.B., Zhu, T.H., Cramer, C.J., and Truhlar, D.G. (1998). New class IV charge model for extracting accurate partial charges from wave functions. *J. Phys. Chem. A* 102, 1820–1831.
36. Chou, T.C. (1974). Relationships between inhibition constants and fractional inhibition in enzyme-catalyzed reactions with different numbers of reactants, different reaction-mechanisms, and different types and mechanisms of inhibition. *Mol. Pharmacol.* 10, 235–247.
37. McGovern, S.L., Caselli, E., Grigorieff, N., and Shoichet, B.K. (2002). A common mechanism underlying promiscuous inhibi-

- tors from virtual and high-throughput screening. *J. Med. Chem.* **45**, 1712–1722.
38. Otwinowski, Z., and Minor, W. (1997). Processing of X-ray diffraction data collected in oscillation mode. *Methods Enzymol.* **276**, 307–326.
  39. Brunger, A.T., Adams, P.D., Clore, G.M., DeLano, W.L., Gros, P., Grosse-Kunstleve, R.W., Jiang, J.S., Kuszewski, J., Nilges, M., Pannu, N.S., et al. (1998). Crystallography and NMR system: a new software suite for macromolecular structure determination. *Acta Crystallogr. D Biol Crystallogr.* **54**, 905–921.
  40. Jones, T.A., Zou, J.Y., Cowan, S.W., and Kjeldgaard, M. (1991). Improved methods for building protein models in electron-density maps and the location of errors in these models. *Acta Crystallogr. A* **47**, 110–119.
  41. Evans, S.V. (1993). SETOR: hardware-lighted three-dimensional solid model representations of macromolecules. *J. Mol. Graph.* **11**, 134–138.

#### Accession Numbers

The structure of AmpC/1 has been deposited with the Protein Data Bank as 1L2S.